Probing many-body localization by excited-state variational quantum eigensolver

Shuo Liu [1,2] Shi-Xin Zhang,[1,2,*] Chang-Yu Hsieh [2,†] Shengyu Zhang,[2] and Hong Yao [1,‡]
[1]*Institute for Advanced Study, Tsinghua University, Beijing 100084, China*
[2]*Tencent Quantum Laboratory, Tencent, Shenzhen, Guangdong 518057, China*

(Received 23 January 2022; revised 16 December 2022; accepted 23 December 2022; published 30 January 2023)

Nonequilibrium physics including many-body localization (MBL) has attracted increasing attentions, but theoretical approaches of reliably studying nonequilibrium properties remain quite limited. In this Letter, we propose a systematic approach to probe MBL phases via the excited-state variational quantum eigensolver (VQE) and demonstrate convincing results of MBL on a quantum hardware, which we believe paves a promising way for future simulations of nonequilibrium systems beyond the reach of classical computations in the noisy intermediate-scale quantum (NISQ) era. Moreover, the MBL probing protocol based on excited-state VQE is NISQ-friendly, as it can successfully differentiate the MBL phase from thermal phases with relatively shallow quantum circuits, and it is also robust against the effect of quantum noises.

DOI: 10.1103/PhysRevB.107.024204

Introduction. Many-body localization (MBL) is a novel dynamical phenomenon occurring in isolated many-body quantum systems. It has long been established that the quantum systems may enter MBL phases in the presence of sufficiently strong random disorder [1–11] or quasiperiodic (QP) potential [12–17] in one-dimensional (1D) systems. In MBL phases, the system fails to thermally equilibrate and exhibits exotic behaviors, such as "area law" entanglement for highly excited states [8–10], logarithmic spread of entanglement [7], and emergent local integrals of motion [10,11]. Such exotic nonequilibrium phases are qualitatively different from thermal phases that are often associated with the eigenstate thermalization hypothesis (ETH) [18–22] and exhibit "volume law" entanglement in highly excited states [23,24]. However, various aspects of MBL remain elusive so far; for instance, whether MBL phases can survive in more than one dimensions is still under debate considering nonperturbative avalanche mechanism [25–27].

To advance our understanding of nonequilibrium quantum phases, it is crucial to unambiguously detect and characterize possible MBL phases for various systems. Numerically, one can probe MBL by calculating the entanglement entropy or level statistics for eigenstates of a Hamiltonian via exact diagonalization, or directly simulating dynamical signatures such as charge imbalance or logarithmic entanglement spreading, following a quantum quench with time-evolution methods. But, existing numerical approaches are often severely restricted due to the exponential scaling of Hilbert space as well as the excessively long evolution time required to simulate steady-state behaviors. Turning to experimental investigations, current hardware platforms still face many challenges, such as short coherence time and limited controllability for the Hamiltonian engineering. That whether MBL exists in more general systems, for example, higher dimensional systems [28–31], has not been rigorously established from current numerical simulations or analog-simulation based experiments.

Quantum computer naturally helps as it can potentially simulate large quantum systems, beyond the capability of classical computers. A common approach is to directly simulate the time evolution of a quantum system using a quantum circuit and determine whether the system will thermalize after a long time by measuring dynamic observables such as charge imbalance. However, currently such an idea is not NISQ-friendly since the required simulation time to confirm the existence of MBL can be much longer than the coherence time of the currently available quantum hardware. Namely, we are faced with the same challenge as other analog experiments without quantum error corrections. Instead, here we propose a more NISQ-friendly approach to detect MBL, relying less on quantum hardware resources and being more robust against noises in quantum hardware.

In this Letter, we propose a general MBL-probing protocol basing on variational quantum algorithms (VQAs). Recently, various quantum-classical hybrid variational algorithms, such as variational quantum eigensolver [32] and quantum approximate optimization algorithm (QAOA) [33–36], which are tailored for the NISQ hardware [37–39], have been proposed. VQE is not only a representative of VQA but also holds great potentials for near-term applications. For different practical problems encoded in VQE, we can define different objective functions (also known as cost functions), and the solutions are expected to give the minimum objective function. For ground state (lowest eigenstate) preparation for a Hamiltonian H, the objective function is defined as the expectation value of H. Firstly, we will generate a trial state $|\psi(\theta)\rangle = U(\theta)|\psi_0\rangle$ to approximate the solution, where $|\psi_0\rangle$ is a given initial state and $U(\theta)$ is an unitary matrix represented by the parameterized quantum circuit (PQC) as shown in Fig. 1. When the PQC is deep enough, the ground state can be exactly written

*shixinzhang@tencent.com
†kimhsieh@tencent.com
‡yaohong@tsinghua.edu.cn

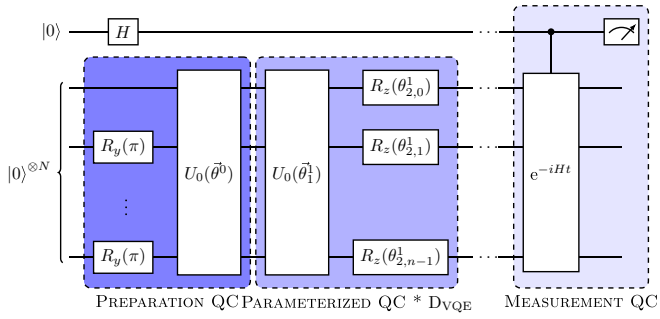

FIG. 1. The circuit structure for the excited-state VQE and eigenstate witness measurement. In preparation circuit part, we first prepare an antiferromagnetic (AF) state $|0101...\rangle$ from the initial state $|0000...\rangle$ and then apply one layer of two-qubit entangling gates to generate the input state $|\psi_0\rangle$ for the PQC. The layer of two-qubit entangling gates is denoted as $U_0(\vec{\theta}^0)$ and $U_0(\vec{\theta}^0) = \prod_{j=0}^{N-1} \exp(\frac{i\pi\theta^0_j}{4}(\sigma^x_j\sigma^x_{j+1} + \sigma^y_j\sigma^y_{j+1}))$. We assume two-qubit entangling gates on different qubits sharing the same weight θ^0 for simplicity. In the PQC part, each block of the ansatz is defined as $U(\vec{\theta}^k) = (\prod_{j=0}^{N-1} \mathrm{Rz}(\theta^k_{2,j}))U_0(\vec{\theta}^k_1)$, which respects $U(1)$ symmetry. Two-qubit entangling gates on different qubits have different weights. The depth of the PQC (number of blocks) D_{VQE} can be adjusted.

as $|\psi(\theta)\rangle$ for suitable parameters. Then, by updating the parameters in shallow PQC based on gradient descent, we will find a final converged state $|\psi(\theta)\rangle$ whose objective function can not decrease anymore and $|\psi(\theta)\rangle$ will be the approximate ground state. The VQE has been exploited in a variety of contexts from quantum chemistry [40–45] and many-body physics [34,46–52], to lattice gauge theories [53,54].

VQE can also be customized to search for excited states. There are several proposals utilizing VQE to discover low-lying excited states of quantum many-body systems, such as orthogonality constrained VQE [55–58], which adds penalty projector terms to the Hamiltonian cost function that project out lower energy states, and subspace expansion method [59,60], which prepares variational states that span the low-energy manifold. Furthermore, VQE can be adapted to search for highly excited states. The objective functions utilized in this case are either the energy variance $C(\theta) = \langle H^2\rangle - \langle H\rangle^2$ [61–69], which only vanishes for eigenstates of H and is greater than zero for the superposition of different eigenstates of H (see the Supplemental Material (SM) for details [70]), or $\langle (H-\lambda)^2\rangle$ [32,34,71–73], which specifically targets an excited state closest to the energy λ. The many-body spectrum can be reconstructed by scanning through a range of λ values within the energy width of H.

In this Letter, we propose to use the excited-state VQE with the energy-variance objective function to detect MBL phases. If the circuit ansatz is deep enough and with sufficient expressivity, then the converged state should be an eigenstate of the system. One can then measure the quantum state to infer purity or real-space inverse participation ratio (IPR) [74,75] as the indicators of MBL phases. This option is straightforward, but it requires a (possibly exponentially) deep and coherent quantum circuit beyond the NISQ regime. We propose an alternative approach, where only the excited-state VQE with a NISQ compatible ansatz is required. In this case, the converged state is not necessarily an eigenstate, especially on the thermal side, where the eigenstate manifests "volume law" entanglement and may not be fully represented with a shallow circuit. Therefore, the indicator to differentiate between MBL and ergodic phases is replaced with the converged performance of the excited-state VQE. On the MBL side, the final state is more quickly converged in terms of the eigenspace distribution. Accordingly, we propose an experimentally measurable quantity that could help assess a state's convergence in the eigenspace. Since our proposed method does not rely on any properties of a particular model, it can be readily applied to a broad range of systems.

Model.—We illustrate the proposed method by investigating the interacting Aubry-André (AA) model [13,15,76–79], a well-studied system hosting the many-body localization transition. The Hamiltonian of the interacting AA model reads:

$$H = \sum_i \left(\sigma^x_i\sigma^x_{i+1} + \sigma^y_i\sigma^y_{i+1} + V_0\sigma^z_i\sigma^z_{i+1}\right) + W\sum_{i=1}^{N}\cos(2\pi\eta i + \phi)\sigma^z_i, \quad (1)$$

where W is the strength of quasiperiodic potential, σ^α are Pauli matrices, N is the size of the system, and ϕ is the phase of the cosine potential. We set $V_0 = 0.5$ and $\eta = (\sqrt{5}-1)/2$ throughout the work. We can numerically determine the MBL transition point via the level spacing ratios for this model [3,80] (see the SM for details [70]).

Circuit ansatz.—Our proposed circuit ansatz for the excited-state VQE consists of two parts: the input-state preparation circuit and the parameterized quantum circuit, acting as the variational ansatz to optimize the cost function, as shown in Fig. 1. Since the AA model conserves the total spin polarization along the z direction, we focus on the total spin $M_z = \sum_i \sigma^z_i = 0$ sector. Namely, the quantum gates employed in the circuit ansatz should respect this $U(1)$ symmetry. The cost function for the excited-state VQE is the energy variance $\langle H^2\rangle - \langle H\rangle^2$, as mentioned before.

Eigenspace inverse participation ratio.—The final converged state $|\psi\rangle$ obtained from the excited-state VQE is a superposition of eigenstates, localized within an energy window, which may not be easily resolved by the energy variance indicator because of the extremely small energy separation between adjacent energy levels (see the SM for details [70]). Theoretically, we may use the eigenspace inverse participation ratio (EIPR) [73] to gauge the extent of convergence onto an eigenstate under the excited-state VQE minimization:

$$\mathrm{EIPR}(|\psi\rangle) = \sum_n |\psi_n|^4, \quad (2)$$

where $|\psi\rangle = \sum_n \psi_n|n\rangle$ and $H|n\rangle = \lambda_n|n\rangle$ with $|n\rangle$ is the nth eigenstate of the Hamiltonian H. For each exact eigenstate of H, its EIPR is one. For a state which is a linear superposition of different eigenstates, its EIPR is less than one. For the maximally randomized state in eigenspace $|\psi\rangle = \sum_n \frac{1}{\sqrt{2^N}}|n\rangle$, where 2^N is the dimension of the Hilbert space of the system, $\mathrm{EIPR} = 1/2^N \to 0$ as $N \to \infty$ in the thermodynamic limit. Consequently, EIPR is capable in efficiently determining whether the final converged state is exactly an eigenstate

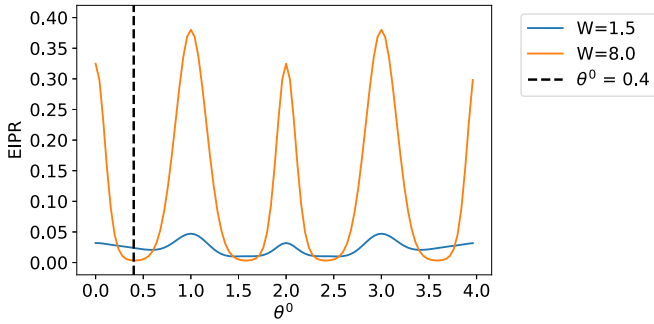

FIG. 2. EIPR of the input state $|\psi_0\rangle$ obtained from the preparation circuit for $W = 1.5$ and 8.0, respectively. Here $N = 12$.

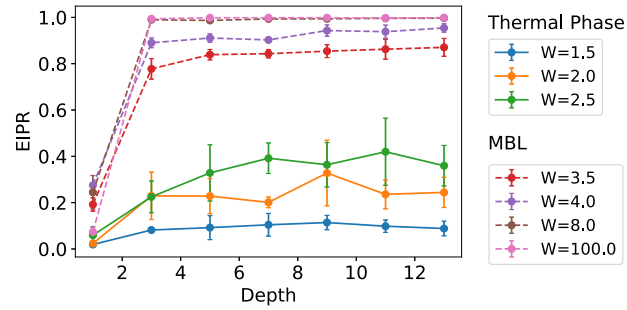

FIG. 3. EIPR of final converged states from excited-state VQE on 12-qubit system with different potential strength W.

of the Hamiltonian H or a superposition of multiple eigenstates.

We firstly investigate the EIPR for the input state $|\psi_0\rangle$, created with the preparation circuit of Fig. 1. The results are shown in Fig. 2. When the system is in the MBL phase ($W = 8.0$), some of the shallow-circuit input states (adjusted by the parameter θ^0) may achieve high EIPR, implying the "area law" entanglement [7–10] for highly-excited eigenstates. On the other hand, when the system is in the thermal phase ($W = 1.5$), all input states consistently score low EIPR, indicating that a shallow circuit has difficulty to approximate the system's eigenstates. Overall, the results shown in Fig. 2 are consistent with the understanding of the AA model. Furthermore, we find a positive correlation between EIPR of input states and EIPR of output states, as well as a positive correlation between energy of input states and energy of output states (see the SM for details [70]). For the following investigations, we then fix $\theta^0 = 0.4$ for input-state preparation. As shown in Fig. 2, the MBL phase has a smaller initial EIPR and the input state's energy is in the middle of energy spectrum in both phases. By this choice, under the excited-state VQE, the output states will likely to converge to some highly excited states, and a high EIPR for output state in MBL phase can be reliably attributed to the nature of the phase instead of a purely better optimization start point.

With the noiseless quantum circuit simulation [81], we calculate EIPR for converged states with varying PQC depth. Theoretically, the expressivity of the variational ansatz increases with the circuit depth, and the achieved EIPR should also improve correspondingly. Indeed, the results for converged states' EIPR, as shown in Fig. 3, support this intuition. Although the initial EIPR of the MBL phase is smaller than that of the thermal phase and the optimization starts from the same input state, the final EIPR of the MBL phase is much larger and extremely close to 1 even with a relatively shallow quantum circuit. There is a clear gap of EIPR between thermal and MBL phases, and the gap grows with system size (see the SM for details [70]). These results confirm that excited-state VQE with shallow circuits indeed performs qualitatively better for MBL systems.

Experimental relevance.—Though EIPR of the output states significantly differs between MBL and thermal phases in numerical simulations, it can not be directly observed in experiments. To determine whether a state is sufficiently enough to reach an eigenstate, an experimentally accessible proxy is desired. To this end, the eigenstate witness [73] is such a quantity which can be experimentally determined via purity measurements. The circuit for eigenstate witness measurement is shown in Fig. 1.

We illustrate the notation of the eigenstate witness as follows. The output state obtained from the excited-state VQE can be written as $|\psi\rangle = \sum_n \alpha_n |n\rangle$, where $|n\rangle$ represents eigenstate of H with eigenenergy λ_n. With an extra ancilla qubit initialized in a superposition state $|+\rangle = (|0\rangle + |1\rangle)/\sqrt{2}$, after a controlled time evolution under H, the reduced density matrix for the ancilla qubit reads:

$$\rho_{\text{reduced}} = \begin{pmatrix} \frac{1}{2} & \frac{1}{2}\sum_n |\alpha_n|^2 e^{i\lambda_n t} \\ \frac{1}{2}\sum_n |\alpha_n|^2 e^{-i\lambda_n t} & \frac{1}{2} \end{pmatrix}, \tag{3}$$

and the eigenstate witness is defined as the purity of the ancilla qubit: $r = \text{Tr}(\rho^2_{\text{reduced}})$, which can be estimated using randomized measurements in experiments [82–84] or a simple state tomography. Such witness is lower bounded by the corresponding EIPR of the output states and can reflect the convergence performance of the excited-state VQE (see the SM for details [70]).

We choose the evolution time $t = 1.0/W$, as the bandwidth is roughly proportional to W. The results of $\ln(1 - r)$ are shown in Fig. 4. For each data point in Fig. 4, the number is averaged over 10 best out of 100 independent optimization results for the excited-state VQE. Both EIPR and r of the MBL phase are larger than those of the thermal phase. These differences will be more prominent as the system size increases.

Theoretically, $\ln(1 - r)$ should approach the minus infinity if the output state is exactly an eigenstate of the system.

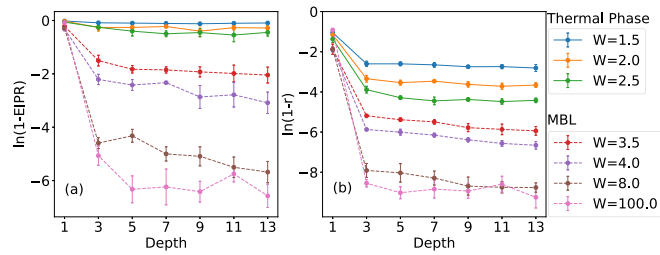

FIG. 4. (a) $\ln(1 - \text{EIPR})$ of final converged states. (b) $\ln(1 - r)$ of final converged states, where r is the eigenstate witness and experimentally accessible. Here $N = 12$.

TABLE I. Fitted circuit depths required to perfectly converge to the excited state for different W.

W	1.5	2.0	2.5	3.5	4.0	8.0
Depths	245	197	256	52	38	14

However, due to the effectiveness of an optimization routine and numerical accuracy of the simulation, the $(1-r)$ value may only reach an "effective zero" from above. In Fig. 4, $(1-\mathrm{EIPR})$ and $(1-r)$ have this effective zero, which is roughly determined by the data from $W=100.0$, supposedly in a deep region of the MBL phase. The effective zero of $(1-r)$ is around -8.9 in the log scale. And the circuit depth required to reach this effective zero depends on Hamiltonian parameter W. We estimate the required depth in Table I [the required depth is fitted by assuming linear relation between $\ln(1-r)$ and the circuit depth]. On the thermal side, the depth required for perfect excited-state convergence is close to 2^N; while on the MBL side, the depth required is in the order of $O(N)$. The depths needed to reach effective zero can serve as another indicator differentiating between the MBL and thermal phases in systems whose phases are unknown. In particular, it is easier to distinguish the two phases when the system size increases.

Effect of quantum noise.—Our approach of probing MBL phases has potential quantum advantage as it can be extended to larger systems and higher dimensions in principle. However, for current quantum computing hardware, we must consider the effects of noise which may compromise the performance of excited-state VQE. One important question is whether we can apply our method to a real device with noises. To answer this question, we carry out similar computation in the presence of a quantum depolarizing channel with noise strength $p=10^{-3}$ after each two-qubit gate. The results are averaged over 5 best of 20 independent trials on an 8-qubit system (the results for larger size systems with the presence of quantum noise obtained by the Monte Carlo trajectory method can be found in the Supplemental Material). As indicated in Fig. 5(a), r does not keep increasing with PQC depths any more; instead, it could decrease due to the accumulated noisy effects for deeper PQC. Nonetheless, the eigenstate witness r behaves sufficiently distinct in the two phases. The magnitude of r from the MBL side is still significantly larger than that from the thermal side. Besides, r shows better noise resilience

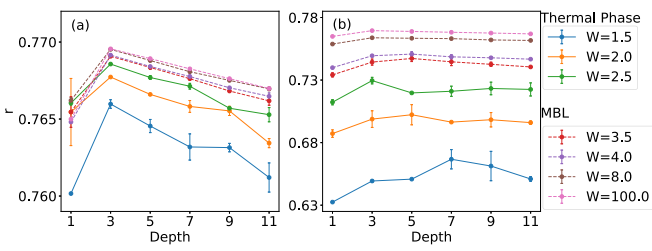

FIG. 5. (a) r of final converged states from a noisy simulation without Trotter decomposition. (b) r of final converged states from a noisy simulation with one time slice Trotter decomposition. Here $N=8$.

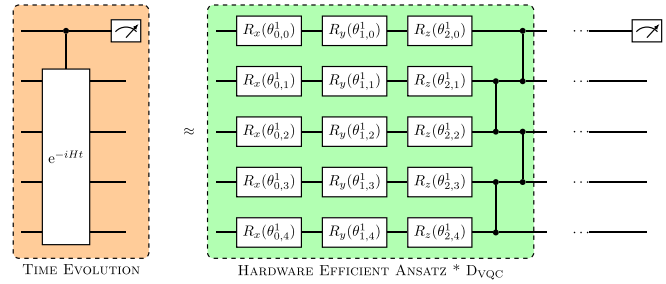

FIG. 6. VQC using hardware-efficient ansatz to approximate controlled time evolution. The two-qubit entangling gate is CZ gate.

when the system enters the MBL side. In the MBL phase, local perturbations spread only logarithmically in time [85], as opposed to the algebraic spreading in thermalizing dynamics. Therefore, r of the thermal phase gets more severely affected due to the faster spreading of quantum noise.

When implementing the controlled time evolution in a real device, one also needs to consider the error brought by the Trotter decomposition. Here we design a type of decomposition that reduces the number of two-qubit gates, and we propagate the system with only one time slice to further reduce the total circuit depth for the digital quantum simulation (see the SM for details [70]). The eigenstate witness r, after incorporating the effects of both noise and Trotter decomposition, is shown in Fig. 5(b), which still behaves distinctly in the two phases. The numerical results confirm that our proposal is NISQ-friendly and ready to be validated in a quantum device.

Real Hardware Experiments.—We apply our method to a four-site model on the available IBM open access quantum hardware. Since the controlled time evolution module is still expensive to implement on NISQ devices [86,87], we further reduce the quantum resources by utilizing a variational quantum circuit (see Fig. 6) to approximate the controlled time evolution module. The VQC is optimized via the normal VQE classically with following cost function:

$$C(\theta)=-\frac{\mathrm{Tr}(U(\theta)V^\dagger)}{2^N}, \tag{4}$$

where $U(\theta)$ is the unitary ansatz of VQC and N is the number of qubits, and

$$V=\begin{pmatrix} I & 0 \\ 0 & e^{iHt} \end{pmatrix}, \tag{5}$$

with the ancilla qubit initialized to $|+\rangle=(|0\rangle+|1\rangle)/\sqrt{2}$ state. Because $U(\theta)V^\dagger$ is also a unitary matrix of dimension 2^N, the cost function has a minimum of -1 when $U(\theta)=V$. We can use $U(\theta)$ as the ansatz to approximate the controlled time evolution in the real hardware. Such a variational circuit is constructed via the hardware-efficient ansatz and thus has less number of two-qubit gates in total while maintaining a high fidelity against the exact controlled time evolution (see the Supplemental Material for more detail). For large system sizes, the loss function defined above is hard to simulate. However, the unitary U to approximate the controlled time evolution module V can also be obtained based on quantum-assisted quantum compiling (QAQC) algorithm with

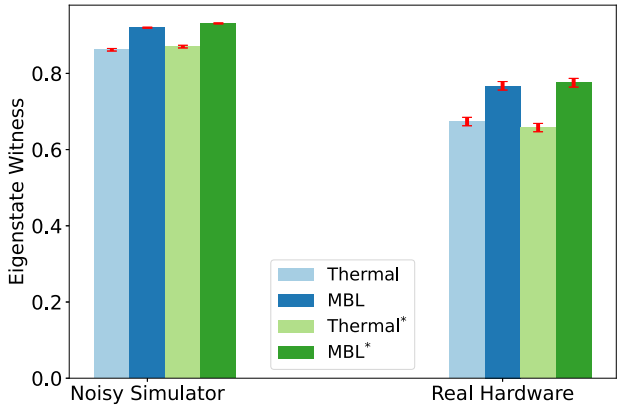

FIG. 7. Eigenstate witness measured on the noisy simulator and real hardware (IBM_Santiago) (in the inset * means the results are processed with readout error mitigation). The estimation error bars due to finite shots of measurement are also included.

an alternative loss function using the Local Hilbert-Schmit Test (LHST) [88], which has better scalability and less barren plateau effect. Therefore, we can carry out the optimization on real quantum hardware when the system size is too large to simulate *in silico*, i.e., we trade off the depth of the time evolution circuit with a large number of shallower variational circuit execution on real devices to make our scheme more suitable on NISQ devices.

We demonstrate our method in a noisy hardware simulator based on IBMQ hardware device (specifically we use the IBM_Santiago instance). We set $W = 8.0$ for the MBL phase and $W = 1.5$ for the thermal phase, and we choose the evolved time $t = 0.15/W$. The parameters of the excited-state VQE and VQC are both determined by the best of 20 independent VQE trials. In Fig. 7, the results of the noisy simulator are the average of $100 * 8192$ independent measurement shots and the results of real hardware are the average of $50 * 8192$ independent measurement shots. A qualitative difference is clearly seen which is sufficient to distinguish the two phases. In fact, for this case, the difference obtained in quantum hardware experiments is even more evident than that obtained from the noisy simulation.

Discussions and concluding remarks.—We have demonstrated that the excited-state VQE with EIPR constitutes a reliable method to probe MBL phase. Since this proposed method requires only a shallow circuit, it can be executed on NISQ hardware when we substitute the EIPR with the eigenstate witness protocol. It is worth noting that though we can use a variational quantum circuit to approximate the controlled time evolution module in principle, this approximation is still challenging on a real NISQ device due to the variational optimization methodology and the depth required for the variational circuit replacement to achieve satisfying fidelity. Still, compared to the conventional approaches that characterize the MBL phase with late-time dynamics, the evolution time required in our method is much shorter and is more compatible with the current-generation quantum computers.

There are many promising directions for further studies. In the present work we have considered only one circuit ansatz. Other different PQC ansatz for excited-state VQE can also be systematically examined for potential benefits. The circuit ansatz with better expressiveness may characterize the highly excited states better, and the optimal ansatz can be automatically designed via techniques from quantum architecture search [89,90]. We can also utilize post-processing enhancements [91] which hopefully improve the performance of excited-state VQE. As our method is independent of the microscopic details of the model considered in this work, it can be straightforwardly extended to investigate other models which might host many-body localization transitions. Moreover, our method can hopefully investigate whether MBL phases can survive in higher dimensions in the future, once the quantum hardware can offer longer coherence time.

Acknowledgements. We thank Z.-Q. Wan for helpful discussions. This work is supported in part by the Beijing Natural Science Foundation under Grant No. Z180010 (H.Y.), the NSFC under Grant No. 11825404 (S.-X.Z., S.L., and H.Y.), the CAS Strategic Priority Research Program under Grant No. XDB28000000 (H.Y.), and Beijing Municipal Science and Technology Commission under Grant No. Z181100004218001 (H.Y.).

[1] I. V. Gornyi, A. D. Mirlin, and D. G. Polyakov, Interacting Electrons In Disordered Wires: Anderson Localization And Low-*t* Transport, Phys. Rev. Lett. **95**, 206603 (2005).

[2] D. M. Basko, I. L. Aleiner, and B. L. Altshuler, Metal-insulator transition in a weakly interacting many-electron system with localized single-particle states, Ann. Phys. **321**, 1126 (2006).

[3] V. Oganesyan and D. A. Huse, Localization of interacting fermions at high temperature, Phys. Rev. B **75**, 155111 (2007).

[4] M. Žnidarič, T. Prosen, and P. Prelovšek, Many-body localization in the heisenberg *xxz* magnet in a random field, Phys. Rev. B **77**, 064426 (2008).

[5] C. Monthus and T. Garel, Many-body localization transition in a lattice model of interacting fermions: Statistics of renormalized hoppings in configuration space, Phys. Rev. B **81**, 134202 (2010).

[6] E. Cuevas, M. Feigel'man, L. Ioffe, and M. Mezard, Level statistics of disordered spin-1/2 systems and its implications for materials with localized Cooper pairs, Nat. Commun. **3**, 1128 (2012).

[7] J. H. Bardarson, F. Pollmann, and J. E. Moore, Unbounded Growth Of Entanglement In Models Of Many-Body Localization, Phys. Rev. Lett. **109**, 017202 (2012).

[8] R. Vosk and E. Altman, Many-Body Localization In One Dimension As A Dynamical Renormalization Group Fixed Point, Phys. Rev. Lett. **110**, 067204 (2013).

[9] M. Serbyn, Z. Papić, and D. A. Abanin, Universal Slow Growth Of Entanglement In Interacting Strongly Disordered Systems, Phys. Rev. Lett. **110**, 260601 (2013).

[10] M. Serbyn, Z. Papić, and D. A. Abanin, Local Conservation Laws And The Structure Of The Many-Body Localized States, Phys. Rev. Lett. **111**, 127201 (2013).

[11] D. A. Huse and V. Oganesyan, A phenomenology of certain many-body-localized systems, Phys. Rev. B **90**, 174202 (2014).
[12] S. Iyer, V. Oganesyan, G. Refael, and D. A. Huse, Many-body localization in a quasiperiodic system, Phys. Rev. B **87**, 134202 (2013).
[13] R. Modak and S. Mukerjee, Many Body Localization In The Presence Of A Single Particle Mobility Edge, Phys. Rev. Lett. **115**, 230401 (2015).
[14] S.-X. Zhang and H. Yao, Universal Properties Of Many-Body Localization Transitions In Quasiperiodic Systems, Phys. Rev. Lett. **121**, 206601 (2018).
[15] T. Kohlert, S. Scherg, X. Li, H. P. Lüschen, S. Das Sarma, I. Bloch, and M. Aidelsburger, Observation Of Many-Body Localization In A One-Dimensional System With A Single-Particle Mobility Edge, Phys. Rev. Lett. **122**, 170403 (2019).
[16] S.-X. Zhang and H. Yao, Strong and Weak Many-Body Localizations, arXiv:1906.00971
[17] S. Ghosh, J. Gidugu, and S. Mukerjee, Transport in the nonergodic extended phase of interacting quasiperiodic systems, Phys. Rev. B **102**, 224203 (2020).
[18] J. M. Deutsch, Quantum statistical mechanics in a closed system, Phys. Rev. A **43**, 2046 (1991).
[19] M. Srednicki, Chaos and quantum thermalization, Phys. Rev. E **50**, 888 (1994).
[20] M. Rigol, V. Dunjko, and M. Olshanii, Thermalization and its mechanism for generic isolated quantum systems, Nature (London) **452**, 854 (2008).
[21] L. D'Alessio, Y. Kafri, A. Polkovnikov, and M. Rigol, From quantum chaos and eigenstate thermalization to statistical mechanics and thermodynamics, Adv. Phys. **65**, 239 (2016).
[22] J. M. Deutsch, Eigenstate thermalization hypothesis, Rep. Prog. Phys. **81**, 082001 (2018).
[23] J. M. Deutsch, Thermodynamic entropy of a many-body energy eigenstate, New J. Phys. **12**, 075021 (2010).
[24] J. R. Garrison and T. Grover, Does A Single Eigenstate Encode The Full Hamiltonian? Phys. Rev. X **8**, 021026 (2018).
[25] W. De Roeck and F. m. c. Huveneers, Stability and instability towards delocalization in many-body localization systems, Phys. Rev. B **95**, 155129 (2017).
[26] T. Thiery, F. m. c. Huveneers, M. Müller, and W. De Roeck, Many-Body Delocalization As A Quantum Avalanche, Phys. Rev. Lett. **121**, 140601 (2018).
[27] I.-D. Potirniche, S. Banerjee, and E. Altman, Exploration of the stability of many-body localization in $d > 1$, Phys. Rev. B **99**, 205149 (2019).
[28] J.-y. Choi, S. Hild, J. Zeiher, P. Schauß, A. Rubio-Abadal, T. Yefsah, V. Khemani, D. A. Huse, I. Bloch, and C. Gross, Exploring the many-body localization transition in two dimensions, Science **352**, 1547 (2016).
[29] P. Bordia, H. P. Lüschen, S. S. Hodgman, M. Schreiber, I. Bloch, and U. Schneider, Coupling Identical One-Dimensional Many-Body Localized Systems, Phys. Rev. Lett. **116**, 140401 (2016).
[30] P. Bordia, H. Lüschen, S. Scherg, S. Gopalakrishnan, M. Knap, U. Schneider, and I. Bloch, Probing Slow Relaxation and Many-Body Localization in Two-Dimensional Quasiperiodic Systems, Phys. Rev. X **7**, 041047 (2017).
[31] T. B. Wahl, A. Pal, and S. H. Simon, Signatures of the many-body localized regime in two dimensions, Nat. Phys. **15**, 164 (2019).
[32] A. Peruzzo, J. McClean, P. Shadbolt, M.-H. Yung, X.-Q. Zhou, P. J. Love, A. Aspuru-Guzik, and J. L. O'Brien, A variational eigenvalue solver on a quantum processor, Nat. Commun. **5**, 4213 (2014).
[33] E. Farhi, J. Goldstone, and S. Gutmann, A Quantum Approximate Optimization Algorithm, arXiv:1411.4028.
[34] J. R. McClean, J. Romero, R. Babbush, and A. Aspuru-Guzik, The theory of variational hybrid quantum-classical algorithms, New J. Phys. **18**, 023023 (2016).
[35] Z. Wang, S. Hadfield, Z. Jiang, and E. G. Rieffel, Quantum approximate optimization algorithm for MaxCut: A fermionic view, Phys. Rev. A **97**, 022304 (2018).
[36] L. Zhou, S.-T. Wang, S. Choi, H. Pichler, and M. D. Lukin, Quantum Approximate Optimization Algorithm: Performance, Mechanism, and Implementation on Near-Term Devices, Phys. Rev. X **10**, 021067 (2020).
[37] M. Cerezo, A. Arrasmith, R. Babbush, S. C. Benjamin, S. Endo, K. Fujii, J. R. McClean, K. Mitarai, X. Yuan, L. Cincio, and P. J. Coles, Variational quantum algorithms, Nat. Rev. Phys. **3**, 625 (2021).
[38] K. Bharti, A. Cervera-Lierta, T. H. Kyaw, T. Haug, S. Alperin-Lea, A. Anand, M. Degroote, H. Heimonen, J. S. Kottmann, T. Menke, W.-K. Mok, S. Sim, L.-C. Kwek, and A. Aspuru-Guzik, Noisy intermediate-scale quantum (NISQ) algorithms, Rev. Mod. Phys. **94**, 015004 (2022).
[39] S. Endo, Z. Cai, S. C. Benjamin, and X. Yuan, Hybrid quantum-classical algorithms and quantum error mitigation, J. Phys. Soc. Jpn. **90**, 032001 (2021).
[40] P. J. J. O'Malley, R. Babbush, I. D. Kivlichan, J. Romero, J. R. McClean, R. Barends, J. Kelly, P. Roushan, A. Tranter, N. Ding, B. Campbell, Y. Chen, Z. Chen, B. Chiaro, A. Dunsworth, A. G. Fowler, E. Jeffrey, A. Megrant, J. Y. Mutus, C. Neill, C. Quintana, D. Sank, A. Vainsencher, J. Wenner, T. C. White, P. V. Coveney, P. J. Love, H. Neven, A. Aspuru-Guzik, and J. M. Martinis, Scalable Quantum Simulation of Molecular Energies, Phys. Rev. X **6**, 031007 (2016).
[41] A. Kandala, A. Mezzacapo, K. Temme, M. Takita, M. Brink, J. M. Chow, and J. M. Gambetta, Hardware-efficient variational quantum eigensolver for small molecules and quantum magnets, Nature (London) **549**, 242 (2017).
[42] J. I. Colless, V. V. Ramasesh, D. Dahlen, M. S. Blok, M. E. Kimchi-Schwartz, J. R. McClean, J. Carter, W. A. de Jong, and I. Siddiqi, Computation Of Molecular Spectra On A Quantum Processor With An Error-Resilient Algorithm, Phys. Rev. X **8**, 011021 (2018).
[43] V. Armaos, D. A. Badounas, and P. Deligiannis, Computational Chemistry on Quantum Computers: Ground state estimation, arXiv:1907.00362.
[44] H. R. Grimsley, S. E. Economou, E. Barnes, and N. J. Mayhall, An adaptive variational algorithm for exact molecular simulations on a quantum computer, Nat. Commun. **10**, 3007 (2019).
[45] J. Tilly, G. Jones, H. Chen, L. Wossnig, and E. Grant, Computation of molecular excited states on IBM quantum computers using a discriminative variational quantum eigensolver, Phys. Rev. A **102**, 062425 (2020).

[46] D. Wecker, M. B. Hastings, and M. Troyer, Progress towards practical quantum variational algorithms, Phys. Rev. A **92**, 042303 (2015).
[47] P.-L. Dallaire-Demers, J. Romero, L. Veis, S. Sim, and A. Aspuru-Guzik, Low-depth circuit ansatz for preparing correlated fermionic states on a quantum computer, Quantum Sci. Technol. **4**, 045005 (2019).
[48] W. W. Ho and T. H. Hsieh, Efficient variational simulation of non-trivial quantum states, SciPost Phys. **6**, 029 (2019).
[49] J.-G. Liu, Y.-H. Zhang, Y. Wan, and L. Wang, Variational quantum eigensolver with fewer qubits, Phys. Rev. Res. **1**, 023025 (2019).
[50] Z. Cai, Resource Estimation for Quantum Variational Simulations of the Hubbard Model, Phys. Rev. Appl. **14**, 014059 (2020).
[51] A. Uvarov, J. Biamonte, and D. Yudin, Variational quantum eigensolver for frustrated quantum systems, Phys. Rev. B **102**, 075104 (2020).
[52] S. Tamiya, S. Koh, and Y. O. Nakagawa, Calculating nonadiabatic couplings and Berry's phase by variational quantum eigensolvers, Phys. Rev. Res. **3**, 023244 (2021).
[53] N. Klco, E. F. Dumitrescu, A. J. McCaskey, T. D. Morris, R. C. Pooser, M. Sanz, E. Solano, P. Lougovski, and M. J. Savage, Quantum-classical computation of schwinger model dynamics using quantum computers, Phys. Rev. A **98**, 032331 (2018).
[54] C. Kokail, C. Maier, R. van Bijnen, T. Brydges, M. K. Joshi, P. Jurcevic, C. A. Muschik, P. Silvi, R. Blatt, C. F. Roos, and P. Zoller, Self-verifying variational quantum simulation of the lattice schwinger model, Nature (London) **569**, 355 (2019).
[55] H. Buhrman, R. Cleve, J. Watrous, and R. de Wolf, Quantum Fingerprinting, Phys. Rev. Lett. **87**, 167902 (2001).
[56] L. Cincio, Y. Subasi, A. T. Sornborger, and P. J. Coles, Learning the quantum algorithm for state overlap, New J. Phys. **20**, 113022 (2018).
[57] O. Higgott, D. Wang, and S. Brierley, Variational quantum computation of excited states, Quantum **3**, 156 (2019).
[58] T. Jones, S. Endo, S. McArdle, X. Yuan, and S. C. Benjamin, Variational quantum algorithms for discovering hamiltonian spectra, Phys. Rev. A **99**, 062304 (2019).
[59] J. R. McClean, M. E. Kimchi-Schwartz, J. Carter, and W. A. de Jong, Hybrid quantum-classical hierarchy for mitigation of decoherence and determination of excited states, Phys. Rev. A **95**, 042308 (2017).
[60] K. M. Nakanishi, K. Mitarai, and K. Fujii, Subspace-search variational quantum eigensolver for excited states, Phys. Rev. Res. **1**, 033062 (2019).
[61] J. H. Bartlett, J. J. Gibbons, and C. G. Dunn, The normal helium atom, Phys. Rev. **47**, 679 (1935).
[62] C. J. Umrigar, K. G. Wilson, and J. W. Wilkins, Optimized Trial Wave Functions For Quantum Monte Carlo Calculations, Phys. Rev. Lett. **60**, 1719 (1988).
[63] L. Marotta and F. Siringo, A variational method from the variance of energy, The European Physical Journal C **44**, 293 (2005).
[64] C. J. Umrigar and C. Filippi, Energy and Variance Optimization of Many-Body Wave Functions, Phys. Rev. Lett. **94**, 150201 (2005).
[65] V. Khemani, F. Pollmann, and S. Sondhi, Obtaining Highly Excited Eigenstates of Many-Body Localized Hamiltonians by the Density Matrix Renormalization Group Approach, Phys. Rev. Lett. **116**, 247204 (2016).
[66] F. Pollmann, V. Khemani, J. I. Cirac, and S. L. Sondhi, Efficient variational diagonalization of fully many-body localized Hamiltonians, Phys. Rev. B **94**, 041116(R) (2016).
[67] F. Vicentini, A. Biella, N. Regnault, and C. Ciuti, Variational Neural-Network Ansatz for Steady States in Open Quantum Systems, Phys. Rev. Lett. **122**, 250503 (2019).
[68] D.-B. Zhang, B.-L. Chen, Z.-H. Yuan, and T. Yin, Variational quantum eigensolvers by variance minimization, Chin. Phys. B **31**, 120301 (2022).
[69] F. Zhang, N. Gomes, Y. Yao, P. P. Orth, and T. Iadecola, Adaptive variational quantum eigensolvers for highly excited states, Phys. Rev. B **104**, 075159 (2021).
[70] See Supplemental Material at http://link.aps.org/supplemental/10.1103/PhysRevB.107.024204 for details, including the following: (1) a brief introduction to level spacing ratio for many-body localization transition, (2) the failure of energy variance to determine the VQE convergence, (3) EIPR and energy correlation between input states and output states of VQE, (4) scaling analysis of EIPR and eigenstate witness, (5) a brief introduction to eigenstate witness, (6) details of quantum noise and Trotter decomposition, (7) details for the real hardware experiments.
[71] J. K. L. MacDonald, On the modified ritz variation method, Phys. Rev. **46**, 828 (1934).
[72] L. Wang and A. Zunger, Solving Schrödinger's equation around a desired energy: Application to silicon quantum dots, J. Chem. Phys. **100**, 2394 (1994).
[73] R. Santagati, J. Wang, A. A. Gentile, S. Paesani, N. Wiebe, J. R. McClean, S. Morley-Short, P. J. Shadbolt, D. Bonneau, J. W. Silverstone, D. P. Tew, X. Zhou, J. L. O'Brien, and M. G. Thompson, Witnessing eigenstates for quantum simulation of Hamiltonian spectra, Sci. Adv. **4**, eaap9646 (2018).
[74] V. Plerou, P. Gopikrishnan, B. Rosenow, L. A. N. Amaral, and H. E. Stanley, Universal And Non-Universal Properties Of Cross-Correlations In Financial Time Series, Phys. Rev. Lett. **83**, 1471 (1999).
[75] P. Pradhan and S. Sridhar, Correlations Due To Localization In Quantum Eigenfunctions Of Disordered Microwave Cavities, Phys. Rev. Lett. **85**, 2360 (2000).
[76] S. Aubry and G. André, Analyticity breaking and anderson localization in incommensurate lattices, Ann. Israel Phys. Soc **3**, 18 (1980).
[77] Y. Lahini, R. Pugatch, F. Pozzi, M. Sorel, R. Morandotti, N. Davidson, and Y. Silberberg, Direct Observation Of A Localization Transition in Quasi-Periodic Photonic Lattices, Phys. Rev. Lett. **103**, 013901 (2009).
[78] J. Biddle, B. Wang, D. J. Priour, and S. Das Sarma, Localization in one-dimensional incommensurate lattices beyond the aubry-andré model, Phys. Rev. A **80**, 021603(R) (2009).
[79] A. Dutta, S. Mukerjee, and K. Sengupta, Many-body localized phase of bosonic dipoles in a tilted optical lattice, Phys. Rev. B **98**, 144205 (2018).
[80] R. E. Throckmorton and S. D. Sarma, Studying many-body localization in exchange-coupled electron spin qubits

using spin-spin correlations, Phys. Rev. B **103**, 165431 (2021).

[81] S.-X. Zhang, J. Allcock, Z.-Q. Wan, S. Liu, J. Sun, H. Yu, X.-H. Yang, J. Qiu, Z. Ye, Y.-Q. Chen, C.-K. Lee, Y.-C. Zheng, S.-K. Jian, H. Yao, C.-Y. Hsieh, and S. Zhang, TensorCircuit: A Quantum Software Framework for the NISQ Era, arXiv:2205.10091.

[82] A. Elben, B. Vermersch, C. F. Roos, and P. Zoller, Statistical correlations between locally randomized measurements: A toolbox for probing entanglement in many-body quantum states, Phys. Rev. A **99**, 052323 (2019).

[83] A. Elben, B. Vermersch, R. van Bijnen, C. Kokail, T. Brydges, C. Maier, M. K. Joshi, R. Blatt, C. F. Roos, and P. Zoller, Cross-Platform Verification Of Intermediate Scale Quantum Devices, Phys. Rev. Lett. **124**, 010504 (2020).

[84] T. Haug, C. N. Self, and M. S. Kim, Large-scale quantum machine learning, arXiv:2108.01039.

[85] D. A. Abanin, E. Altman, I. Bloch, and M. Serbyn, Colloquium: Many-body localization, thermalization, and entanglement, Rev. Mod. Phys. **91**, 021001 (2019).

[86] K. Mitarai and K. Fujii, Methodology for replacing indirect measurements with direct measurements, Phys. Rev. Res. **1**, 013006 (2019).

[87] K. Bharti and T. Haug, Quantum-assisted simulator, Phys. Rev. A **104**, 042418 (2021).

[88] S. Khatri, R. LaRose, A. Poremba, L. Cincio, A. T. Sornborger, and P. J. Coles, Quantum-assisted quantum compiling, Quantum **3**, 140 (2019).

[89] S.-X. Zhang, C.-Y. Hsieh, S. Zhang, and H. Yao, Differentiable quantum architecture search, Quantum Sci. Technol. **7**, 045023 (2022).

[90] S.-X. Zhang, C.-Y. Hsieh, S. Zhang, and H. Yao, Neural predictor based quantum architecture search, Machine Learning: Science and Technology **2**, 045027 (2021).

[91] S.-X. Zhang, Z.-Q. Wan, C.-K. Lee, C.-Y. Hsieh, S. Zhang, and H. Yao, Variational Quantum-Neural Hybrid Eigensolver, Phys. Rev. Lett. **128**, 120502 (2022).